OPEN ACCESS

International
Journal
Of Modern Engineering Research (IJMER)

Geochemistry and Genesis of Kammatturu Iron Ores of Devagiri Formation, Sandur Schist Belt, Karnataka, India

Veeresh Menasinakai[1], G S Pujar[2]

[1] *Department of Studies in Geology, Karnataka University, Dharwad, Karnataka, INDIA*
[2]*Associate professor, Department of Geology, Karnataka Science College, Dharwad, Karnataka, INDIA*

ABSTRACT: *The Greenstone belts of Karnataka are enriched in BIFs in Dharwar craton, where Iron formations are confined to the basin shelf, clearly separated from the deeper-water iron formation that accumulated at the basin margin and flanking the marine basin. Geochemical data procured in terms of major, trace and REE are plotted in various diagrams to interpret the genesis of BIFs. Al_2O_3, Fe_2O_3 (T), TiO_2, CaO, and SiO_2 abundances and ratios show a wide variation. Ni, Co, Zr, Sc, V, Rb, Sr, U, Th, ΣREE, La, Ce and Eu anomalies and their binary relationships indicate that wherever the terrigenous component has increased, the concentration of elements of felsic such as Zr and Hf has gone up. Elevated concentrations of Ni, Co and Sc are contributed by chlorite and other components characteristic of basic volcanic debris. The data suggest that these formations were generated by chemical and clastic sedimentary processes on a shallow shelf. During transgression, chemical precipitation took place at the sediment-water interface, whereas at the time of regression. Iron ore formed with sedimentary structures and textures in Kammatturu area, in a setting where the water column was oxygenated.*

Key words: *BIFs, clastic, Green stone belts, Kammatturu, terrigenous.*

I. INTRODUCTION

The Sandur schist belt is one of the important schist belts among the five Dharwarian supracrustal belts in the Karnataka Craton of South India, which runs in Bellary-Sandur-Hospet sector. The Dharwar Schist belt marks the transition from Archean to Proterozoic era belonging to the age group of 2900-2600 million years. In India, deposition of BIF is mainly confined to greenstone belts and peak of BIF deposition is found around 2.7 Ga. C. Manikyamba. (1999) (i.e.[16]). The Sandur schist belt covers an area of 960 sq. Km, comprising of Banded Iron formations, shales, phyllites, schists, etc. It is structurally highly disturbed and squeezed out of shape by the intrusion of Younger granites. Comprising of manganiferous greywacke, phyllite and numerous bands of banded hematite quartzites (BHQ) characterize the basin. Reviewing the Banded iron-formation of India, Radhakrishna et al (1986) (i.e.[14]) observed that though there are number of partial major element analyses of iron formations, informations on trace element and REE is scanty. Rare earth element (REE) distribution patterns of Precambrian banded iron-formations have been studied extensively during the last decade (Fryer, 1977 a,b, 1983; Graf, 1978; (i.e.[1]) Appel,1983). The geochemistry of REE is one of the most powerful tools in elucidating either igneous or sedimentary processes (due to the coherent behaviour of REE). It helps in understanding the genesis, source as well as environment of deposition (Fryer, 1983) (i.e.[5]). Information available on REE of BIF of India has been presented by Majumder et al (1984), Chakraborty et al (1986) and geochemistry group, N.G.R.I. for Bihar, Orissa and Karnataka iron formations. Recently Prasad et al (1993) presented the REE distribution pattern for selected iron formations from Tamil Nadu. Overall abundances of REE in the iron formation of India are low, pointing to its early Archaean age. The present work includes the detailed geochemical analysis of litho units from Kammatturu area, in terms of major, trace and REE, and the results obtained are plotted in the binary/ternary diagrams to comment on their genesis and various aspects.

II. GEOLOGY OF SANDUR SCHIST BELT

Sandur schist belt is located at the eastern margin of the Karnataka Nucleus. The lithostratigraphy is correlated with the Bababudan group of the Dharwar Supergroup (Radhakrishna, 1983) (Fig. 1). It rests on 3.0 Ga old gneisses and is intruded by 2.6 Ga granites suggesting that its age may be between 3.0 to 2.6 Ga. Bhaskar Rao, et al., (1992) (i.e.[3]) have estimated Rb/Sr restting ages of 2.4 Ga of various rock types of this belt. In Sandur Schist Belt the iron and Manganese deposits are concentrated along the hilltop and ridges ranging between 600 to 1100 m in altitude. The basin is known for its rich accumulation of iron and partial accumulation of Manganese Ore. The iron and manganese ores are confined to eight mountain ranges (Fig. 2).

III. GEOLOGY OF KAMMATTURU AREA

In Sandur schist belt Iron ores are observed in Devagiri hill ranges, around Kammatturu village (Fig. 2). Kammatturu iron formation is parallel to sub parallel with Donimalai block occurce in Devagiri formation in Sandur schist belt. This Iron ore zone is designated as Kammatturu block-A, B and C in accordance with strike direction ($N50^0W$ – $S50^0E$) dipping 55^0 towards NE. Kammatturu Iron ore formation is hosted by highly disturbed BIFs, manganiferous phyllite, ferruginous shale, metavolcanics. The Iron ores have been classified on their physical characters like Massive hematite ore, Flaky or biscuity ore, Laminated ore, Powdery ore, Laterite ore, Goethite ore, Shaly ore, BHJ, BHQ and BMQ. Fresh BIF and other rock type samples are occurring at and around Kammatturu village of Devagiri formation. This is evidenced by core samples, working mine pits, road cuttings and exposure of the un-weathered deeper parts of different formations.

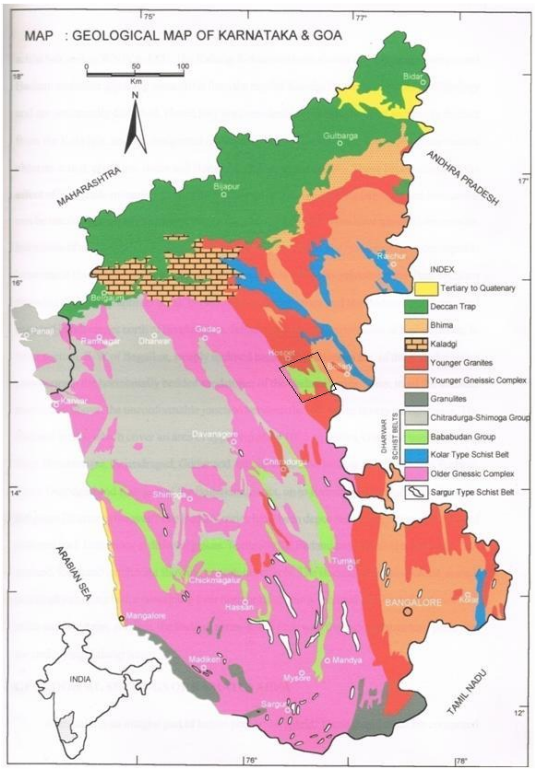

Fig. 1. Geological map of Karnataka

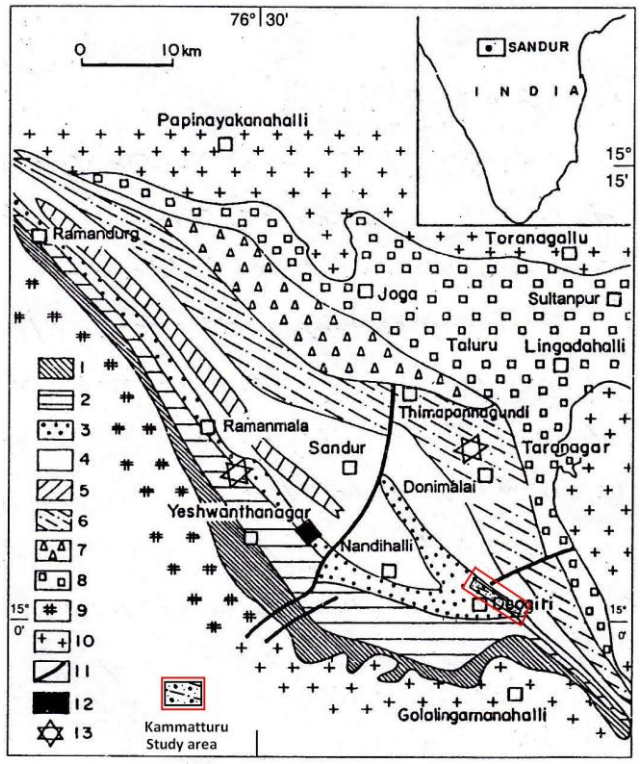

Fig. 2 a) shows the location of Sandur schist belt in Peninsular India, b) shows the simplified map with Kammatturu study area in Sandur schist belt.

Index- 1) Yeshwanthanagar Volcanic Block (YVB), 2) Deogiri Block (DB), 3) Western Volcanic Block (WVB), 4) Central Volcanic Block (CVB), 5) Greywackes in Central Volcanic Block, 6) Eastern Volcanic Block (EVB), 7) North Central Acid Volcanic Block (NCAVB), 8) Sultanpura Volcanic Block (SVB), 9) unclassified gneisses and granites, 10) Granites, 11) fault planes, 12) closed block represents the area where BIF-GIF are exposed and the location of the samples, 13) represents the occurance of BIF at Ramandurg and Donimalai ranges. Last legend red colour square is shown by Author i.e. Kammatturu Study area. Source: C. Manikyamba. (i.e.[16]).

IV. GEOCHEMISTRY

Banded iron formations (BIFs), shaly BIF and shales are found interbedded at the Kammatturu study area of the Sandur schist belt. Cherts and shales are two end members in which deposition of Fe_2O_3 and Al_2O_3 in variable proportions has given rise to observed large-scale variation in major, trace and REE abundances. Based on the composition (wt. %) of SiO_2, Al_2O_3 and Fe_2O_3 content, the samples analysed are grouped as Iron ores, Banded Hematite Quartzite and shales. Samples show mixtures of SiO_2 and Fe_2O_3 are varying from 2.59 to 17.27 and 69.19 to 91.46, respectively in Iron ore samples, 41.30 to 45.97 and 52.09 to 55.47, respectively. Al_2O_3 lies between 0.54 and 0.98 in all the BIFs samples, suggesting a cherty BIF, in two samples Al_2O_3 is between 7.66 - 7.99, which is a shale/shaly BIF. CaO is varying from 0.03 to 0.07, justifying the BIF association with sulphides. Lack of correlation of Al2O3, CaO and alkalies suggests little input of detrital feldspar in the BIF.

Table1: Average chemical composition (Major Oxides) (in wt. %) of BIF samples from the Study area, compared with world standard samples.

	Lake Superior#	Algoma#	Archaean*	Eastern India*	Sandur CBIF□	Kammatturu area ‡
SiO_2	47.20	50.50	47.30	47.02	51.80	43.63
Al_2O_3	1.39	3.00	1.25	0.07	0.23	0.83
$Fe_2O_3^t$	35.40	26.90	22.94	44.16	44.30	53.88
CaO	1.58	1.51	2.84	0.17	0.09	0.04
MgO	1.24	1.53	3.66	0.13	0.15	0.05
MnO	0.73	0.22	0.59	0.06	0.09	0.06
Na_2O	0.12	0.31	0.22	0.10	0.19	0.03
K_2O	0.14	0.58	0.09	0.13	0.07	0.02
P_2O_5	0.06	0.21	0.22	0.07	0.08	0.02

Gross and Mcleod (1980) (i.e.[18]). * Gole and Klein (1981) (i.e.[8]). □ Manikyamba et al., (1993) (i.e.[19]).
‡ BIF samples (average of 8) from Study area – Fusion, Acid digestion and ICP OES Finish.

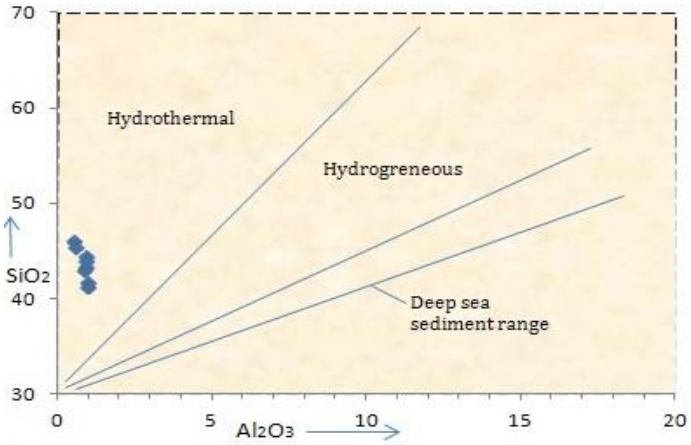

Fig. 3. SiO_2 /Al_2O_3 discrimination diagram for BIF (after Bonatti, 1975)

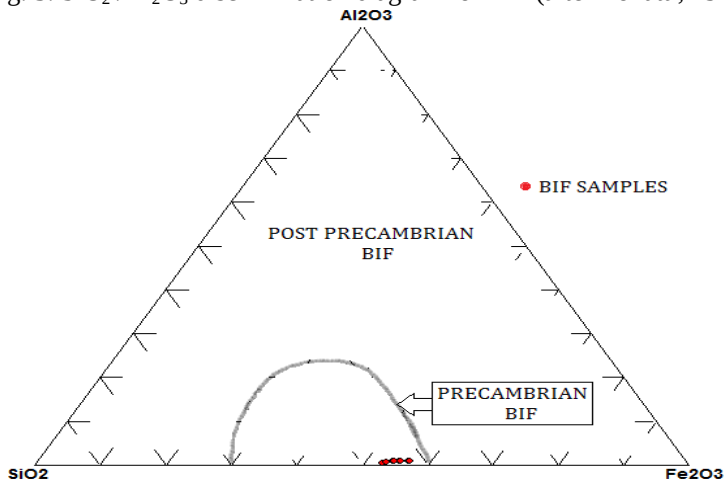

Fig. 4. Ternary plot of SiO_2, Al_2O_3 and FeO, Showing BIF Sample are falling within Precambrian field, (after Govett, 1966).

The results of BIF samples data "Table 1" indicates that major elements like Al_2O_3, CaO, MgO and MnO values are high in Lake Superior, Algoma and Archean type. Iron formation is at least twice that of the Superior facies iron formations (Gross and Mcleod, 1980) (i.e.[18]). The average values of the above elements of the Study area samples are similar to the average values of the Lake Superior, CBIF, Archaean type (Manikyamba et al, 1993) (i.e[19]). All the eight BIF Samples are showing more concentration of Fe_2O_3 and SiO_2 and depleted in CaO, K_2O and P_2O_5. This might be due to the close association with high grade iron ore deposits. Na_2O/K_2O discrimination diagram Fig. 5 (After Smith, 1982) for study area indicating the sedimentary

origin. Al_2O_3, MnO, MgO and CaO indicating carbonate facies of BIF. It is observed that there is no significant variation in respect of any of the elements, with exceptional cases of Cao, MgO and Fe_2O_3.

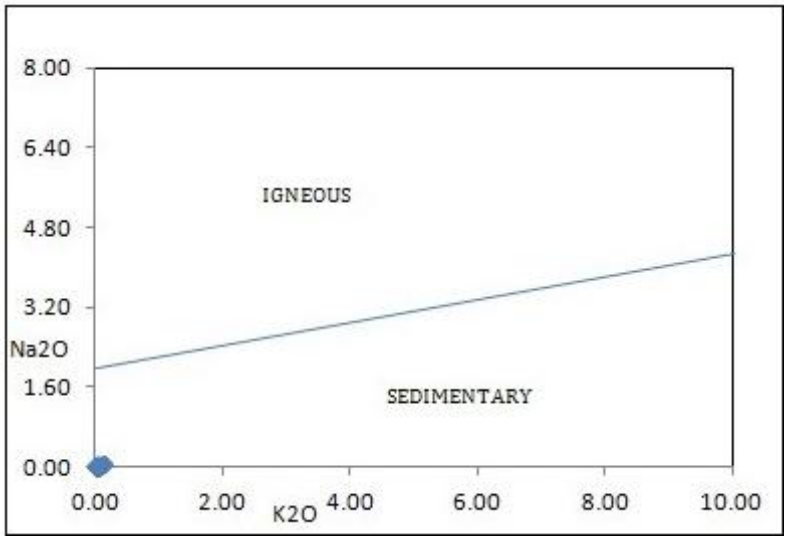

Fig. 5 Na_2O-K_2O variation diagram of Iron Formation from study area, and showing fields of Igneous and sedimentary nature (After Smith, 1982).

BIF samples has 0.03 to 0.06 % TiO_2 with Al_2O_3 values ranging between 0.54 to 0.98 %. In SBIF both the TiO_2 and Al_2O_3 values are elevated from 0.34 to 0.38 % and from 7.66 to 7.99 % respectively. The TiO_2/Al_2O_3 ratio for both types of BIF is always less than one (Fig. 6A). Linear relationships between Al_2O_3 and TiO_2 of S macrobands has been observed by several workers (Ewers and Morris. 1981). In the study area samples we observe similar linearity and slightly scattered at less concentration in (Fig. 6A). This shows clastic input for different layers and at different levels has been inconsistent and may probably represent different types of source rocks. It is indicate that clastic sedimentation from variable compositional sources has also occurred simultaneously with chemical precipitation of SiO_2 and Fe_2O_3.

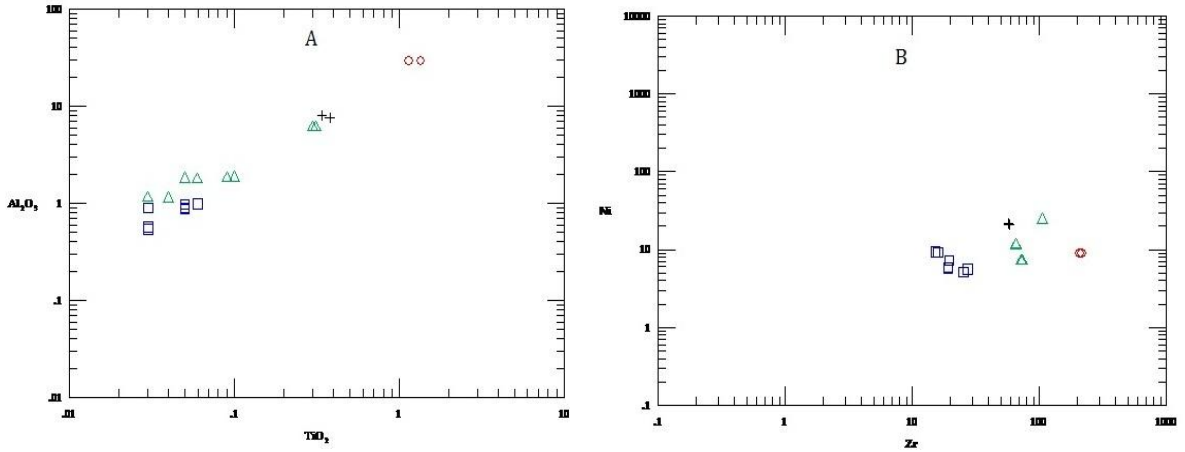

Fig. 6(A). Al_2O_3/TiO_2 variation diagram for Iron formations of Kammatturu. (B) Ni/Zr relationship shows a complete gradation with both scatter and linearity between BIF and Shales. Ref Legend at 6(C).

Ni abundances variation between 5 to 24 ppm and Zr varies from 15 to 217 ppm in the iron formations. A gradual increase of these two elements is seen in BIF and Iron formations (Fig. 6B). Zr abundances of shale, Ferruginous shale are high. The Ni/Zr ratios and behavior demonstrate the clastic contribution to these rocks. Zr may be contributed from terrigenous sediments.

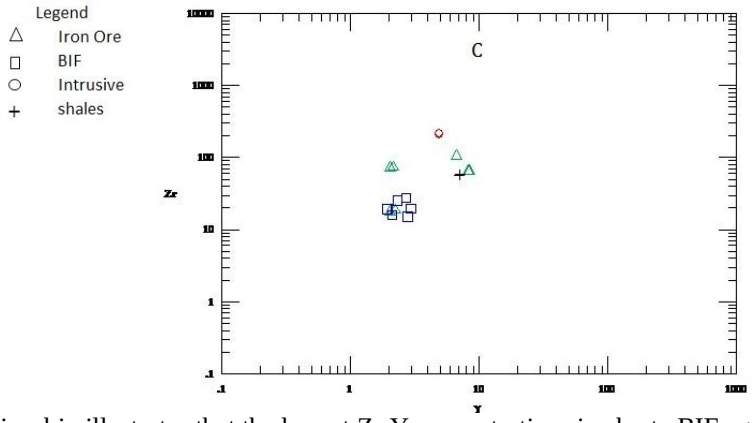

Fig. 6(C). Zr/Y relationship illustrates that the lowest Zr,Y concentrations in cherty BIFs gradually grade into shaly BIF and shales of high Zr and Y abundances.

Elements Zr and Y behaviour in the binary graph (Fig. 6(C) shows a gradual increase of both Zr and Y is observed and also no compositional gap is seen, it suggests that mixing of chemical precipitates and clastics has been the main reason.

Table 2. Chemical composition of Iron Formations from Kammatturu area.

Major elements (wt%)/ Sample code	**KA-1**	**KA-3**	**KA-11**	**KA-13**	**KA-6**	**KA-8**	**KA-16**	**KA-18**	**KA-5**	**KA-10**
SiO_2	5.61	2.69	5.51	2.59	41.70	45.97	41.30	45.33	38.00	24.23
TiO_2	0.04	0.05	0.03	0.06	0.05	0.03	0.06	0.03	1.35	0.38
Al_2O_3	1.12	1.77	1.13	1.75	0.97	0.54	0.98	0.57	29.27	7.66
Fe_2O_3	91.46	90.56	90.46	90.53	55.37	52.09	55.47	52.49	17.72	57.21
MnO	0.006	0.113	0.016	0.103	0.077	0.037	0.075	0.035	0.073	0.074
MgO	0.03	0.02	0.03	0.02	0.03	0.12	0.05	0.10	0.07	0.03
BaO	0.004	0.007	0.004	0.017	0.009	0.004	0.019	0.004	0.005	0.004
CaO	0.03	0.03	0.03	0.03	0.03	0.03	0.07	0.03	0.10	0.06
Na_2O	0.04	0.06	0.05	0.07	0.03	0.03	0.02	0.03	0.07	0.04
K_2O	0.02	0.02	0.02	0.01	0.01	0.01	0.02	0.01	0.06	0.02
P_2O_5	0.03	0.07	0.04	0.06	0.02	0.01	0.03	0.02	0.04	0.15
Cr_2O_3	0.004	0.004	0.004	0.014	0.003	0.004	0.002	0.004	0.018	0.020
LOI	1.55	4.42	1.56	4.43	1.41	1.00	1.40	1.00	12.87	10.06

Trace elements (ppm)/ Sample code	**KA-1**	**KA-3**	**KA-11**	**KA-13**	**KA-6**	**KA-8**	**KA-16**	**KA-18**	**KA-5**	**KA-10**
Co	2.20	7.72	2.13	7.12	5.02	2.90	5.92	2.81	14.70	11.50
Cs	<0.5	<0.5	<0.5	<0.5	0.97	<0.5	1.13	<0.5	0.54	<0.5
Cu	1.90	21.92	2.90	20.92	12.00	10.81	12.45	11.81	172.56	63.41
Ga	0.59	1.93	0.69	1.73	17.09	<0.5	17.19	<0.5	33.61	10.83
Hf	0.86	1.17	0.66	1.17	<0.5	0.66	<0.5	0.62	5.19	1.76
Nb	3.06	2.11	3.02	2.11	1.61	3.23	1.66	3.11	6.82	4.87
Ni	<5	11.40	<5	11.50	9.38	5.78	9.25	5.90	8.84	21.56
Rb	1.02	0.86	1.12	0.81	1.50	3.25	1.45	3.28	3.76	0.36
Sc	2.39	6.75	2.59	6.75	2.39	1.04	2.49	1.14	59.25	13.19
Sr	4.40	5.04	4.60	5.24	4.90	4.61	4.91	4.72	8.85	6.37
V	15.01	21.63	15.91	20.03	14.65	<10	14.95	<10	496.00	147.57
Y	2.05	8.47	2.25	8.31	2.79	1.91	2.11	1.94	4.90	7.04
Zn	232.84	186.77	229.84	188.77	78.37	60.29	78.90	62.29	307.36	307.45
Zr	17.60	65.30	18.60	65.30	15.21	19.27	15.99	19.17	216.82	57.12

REE (ppm)/ Sample code	KA-1	KA-3	KA-11	KA-13	KA-6	KA-8	KA-16	KA-18	KA-5	KA-10
La	1.6	6.6	1.6	6.4	3.4	1.7	3.4	1.8	4.8	6.3
Ce	3.1	8.2	3.0	8.4	6.4	2.6	6.6	2.5	24.1	12.3
Pr	0.34	2.20	0.37	2.19	0.50	0.31	0.52	0.32	1.10	2.13
Nd	1.4	9.2	1.3	9.0	2.2	1.6	2.2	1.9	4.2	8.1
Sm	0.30	2.10	0.39	2.01	0.42	0.26	0.43	0.25	0.88	1.83
Eu	<0.000	0.23	<0.0	0.25	<0.000	<0.000	<0.0	<0.0	<0.000	0.08
Gd	0.28	2.17	0.29	2.07	0.34	0.21	0.33	0.20	0.87	1.70
Tb	0.01	0.27	0.22	0.25	0.00	<0.000	0.20	<0.0	0.14	0.26
Dy	<0.5	2.0	<0.5	2.0	<0.5	<0.5	<0.5	<0.5	1.1	1.8
Ho	0.03	0.33	0.02	0.23	0.04	<0.000	0.03	<0.0	0.23	0.35
Er	0.13	1.10	0.14	1.13	0.17	0.06	0.18	0.13	0.73	1.16
Tm	<0.000	0.1	<0.0	0.1	<0.000	<0.000	<0.0	<0.0	0.1	0.1
Yb	0.15	0.95	0.16	0.96	0.16	0.17	0.12	0.18	0.84	1.11
Lu	<0.000	0.10	<0.0	0.09	<0.000	<0.000	<0.0	<0.0	0.13	0.12
REE	7.3	35.6	7.6	35.2	13.7	6.9	14.0	7.3	39.1	37.4

Out of total samples only 10 are considered here First 4 are IO=Iron Ore, Second 4 are BIF=Banded Iron Formation, Third 1sample is Intrusive and the last 1 is Shale.

Hf and Zr both increase simultaneously Fig. 7(A) shows an excellent linear relationship between the values from IO, BIF, intrusive and shales samples. There is no gap between IO, BIF and shales. This suggests that a continuous supply of varying quantity of the divergent types of terrigenous and volcaniclastic debris has been maintained to the basin and the mixing of hydrothermal solutions with clastics derived from two divergent sources has taken place. Zr, Y and Hf are provided by felsic rocks and if felsic volcanic ash would have provided these elements. In this figure, intrusive rocks exhibit a slight gap from above samples, suggesting the later/younger formations.

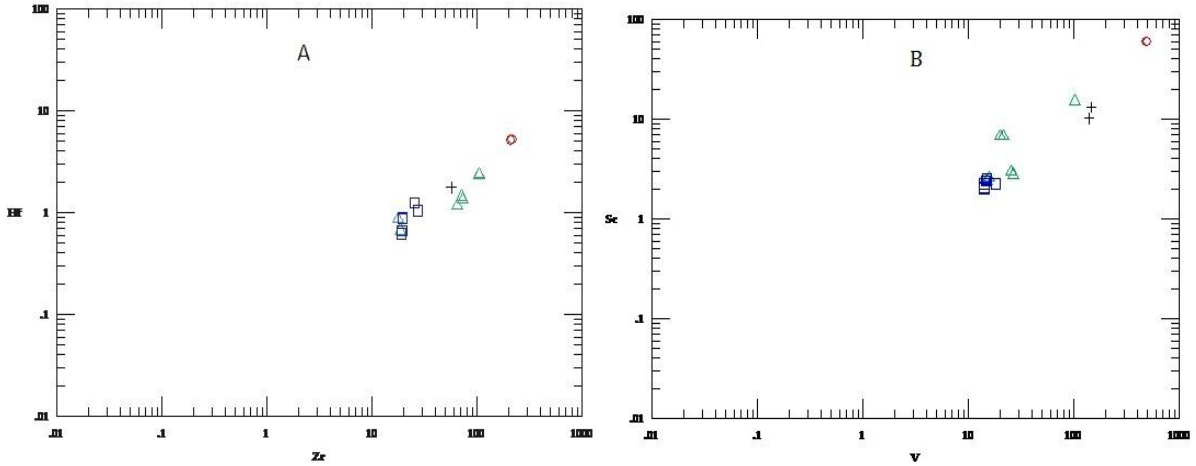

Fig. 7(A) Zr-Hf pattern with a large scale scatter in cherty BIF linearity between shaly BIF samples. (B) Sympathetic linear Sc-V relationship shows small scale scatter. Ref Legend at 6(C)

Maximum enrichment of Sc and V has occurred in Shales and all samples of BIF are extremely depleted in both Sc and V. A complete gradation of BIF into Shales is seen in the Sc - V plot (Fig. 7(B). Similar conjecture is made by C. manikyamba et. al.(1993) (i.e.[19]). Samples indicate a late stage hydrothermal syngenetic emplacement of these elements.

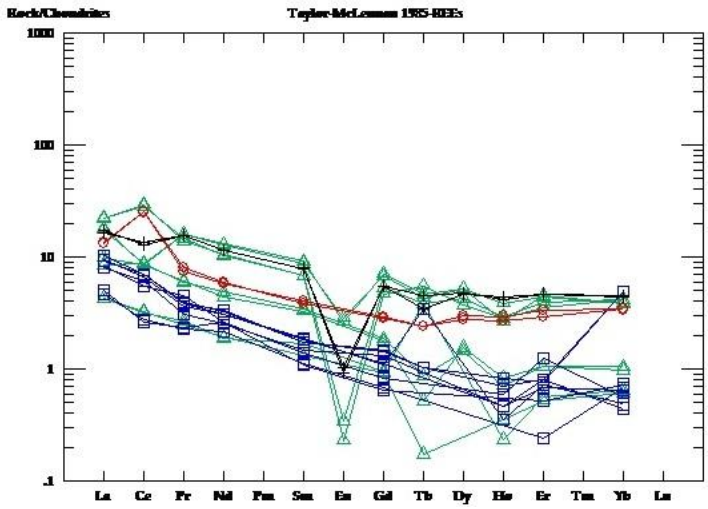

Fig. 8 REE patterns of Iron formation with moderate ∑REE abundances, showing fractionation from La to Lu with variation in Eu anomalies. No La enrichment or Ce depletion is seen in these samples. Ref Legend at 6(C)

Chondrite normalized patterns are shown in Fig. 8 Iron ore, BIF, Intrusive and shales, samples are characterized by moderate ∑REE abundances with average Eu anomaly in BIF, shales. Extremely depleted in iron ore and intrusive samples, $Nd_N/Yb_N>1$ and LREE/HREE>1. Sloping REE patterns due to slight depletion in HREE and average Eu anomaly are characteristic features. No La enrichment and Ce depletion are recorded in this group. The REE content of Kammatturu area BIF shows low to high variation in abundance "Table. 2". Different patterns (Fig. 8) represent the end product of a complex series of events that record the properties of the solutions that precipitated them with clastic sediments. A contemporaneous input of clastic material appears to have greatly affected the absolute abundance of REE in these rocks. The overall shape of the REE patterns of the oxide facies BIF samples comprising only chert and iron minerals is generally similar to patterns of modern sea water, with the exception of La, Ce and Eu which show anomalous behavior. The overall shape of REE patterns depicted here represents the Archaean oxide facies. The inferences enumerated above are in conformity with the observations made by C. Manikyamba et. al.(1993) (i.e.[19]), Derry and Jacobsen (1990).

V. CONCLUSION

The geochemistry of Kammatturu Iron Formations comprising of Iron ore, BIF, shale and intrusive in the form of major, trace and REE is carried out to know the behaviour and patterns of the elements which are represented in Binary and Ternary diagrams to unravel the genesis of litho units. From the foregoing account the following conclusions may be drawn.

1. Iron ore/BIFs are interbedded in the Study area. Cherts and shales are two end members in which mixing of minerals containing Al_2O_3 and Fe_2o_3 in various proportions have given rise the observed compositional variations from cherts to ferruginous cherts, cherty BIF, shales. These variations caused by mixing of volcaniclastic and terrigenous sediments with precipitation of Ni, Cr, Zr, Y, V, Sc, Ti and ∑REE ratios.

2. Volcaniclastic debris are preserved in the high Ni content of Iron ore formations. Terrigenous sedimentation is reflected in , Zr, Y, V, Sc, Hf, Ta and Nb abundances.

3. Maximum samples show depletion in Ce and negative in intrusive samples and two from iron ore samples and indicate oxidation of hydrothermal solutions on stable shelf zones. The magnitude of La enrichment is variable suggesting the mixing of hydrothermal solutions with ambient sea water.

4. On the bases of geochemical data and field evidence it is suggested that the Study area BIFs were deposited by a combination of four processes. Hydrothermal solutions and fluvial solutions provided the SiO2 and FeO and REE of the deposits. The banding of the BIF represents the break in precipitation of iron due to non availability of photosynthetic O_2 or hydrothermal FeO or both. Therefore, processes like (1) Hydrothermal activity in a deeper reducing alkaline environment (2) volcanic/terrigenous sedimentation, (3) oxidation have produced the BIFs of Kammatturu area.

REFERENCES

Journal Papers:

[1]. Graf,J.L.,P.K., 1978. Rare earth elements, iron formations and sea water. Geochim.Cosmochim. Acta, 42: 1845-1850.

[2]. Abbott, D. H. (1996). Plumes and hotspots as sources of greenstone belts. Lithos, v. 37, pp. 113-127.

[3]. Bhaskar Rao, Y.J., Sivaraman, T.V., Pantulu, G.V.C., Gopalan,K. And Naqvi, S.M.,1992. Rb-Sr ages of Late Archaean metavolcanics and granites. Dharwar craton, evidence for Early Protrozoic thermotectonic event(s). Precambrian Res., submitted.

[4]. Gnaneshwar Rao, T. And Naqvi. S.M. (1995). Geochemistry, depositional environment and tectonic setting of the BIF's of the late Archean Chitradurga schist belt, India. Chem. Geol., v. 121.pp.217-243.

[5]. Fryer, B.J.,1983. Rare earth elements in iron formations. In: A.F.Trendall and R.C.Morris(Editors), Iron Formation: Facts and Problems. Elsevier, Amsterdam, pp.345- 358.

[6]. Abbott, D. H., Drury, R. And Smith, W.H.F. (1994). The flat to steep transition in subduction style. Geology,v.22,pp.937-940.

[7]. Fryer, B J., Fyfe, W.S. and Kerrich,R., 1979. Archaean volcanogenic oceans. Chem. Geol., 24; 25-33.

[8]. Gole. M. J. and klein, C., 1981. Banded iron-formations through much of Precambrian time. J. Geol., 89 : 169-183.

[9]. Gross., 1965. Geology of iron deposits in Canada. 1. General geology and evaluation of iron deposits. Geol. Surv. Can.
Econ. Geol. Rep., 22: 181.

[10]. Radhakrishna, B.P.1983. Archaean granite greenstone terrain of South India. In; S.M. Naqvi and J.J.W.Rogers (Editors), Precambrian of South India. Mem. Geol., 94: 145-166.

[11]. Hofmann, A. W. (1996). Mantle geochemistry: the message from oceanic volcanism. Nature,.385, pp.219-229.

[12]. James H L 1954. Sedimentary facies of iron formations; Econ. Geol. 49. 235-293.

[13]. James H L., 1983. Distribution of banded iron-formation in space and time. In: A. F.Trendall and R.C. Morris (Editors), Iron Formation: Facts and Problems. Elsevier, Amesterdam, pp. 471-490.

[14]. Radhakrishna et al (1986) Banded iron-formation of India, J. Geol. Soc. India, 28: 1-28.

[15]. Manikyamba, C. and Naqvi S. M. (1998) Type and processes of greenstone belt formation. In: B. S. Paliwal (Ed.). The Indian Precambrian. Scientific Publishers, Jodhpur, pp.18-32.

[16]. Manikyamba, C. (1999) Reworking of BIF into GIF in the Sandur schist belt, India :Possible evidence of sea level changes in an Archaean proto-ocean. Jour. Geol. Soc. India, Vol. 53, p. 453-461.

[17]. K. S. S.Prasad, Geochemistry and Origin of Banded Iron-Formation from the Granulitic Terrain of North Arcot District, Tamil Nadu, South India. Chem Sci Trans., 2012, 1(3), 482-493.

[18]. Gross, G.A., 1980. Aclassification of iron formation based on depositional environment. Can. Mineral., 18: 215-222.

[19]. Manikyamba, C., Balaram, V. and Naqvi, S.M. (1993) Geochemical signatures of Polygenecity of Banded Iron Formations (BIF) of Archean Sandur greenstone belt (schist belt) Karnataka Nucleus, India. Precambrian Research. Vol. 61. P. 137-164.

[20]. Simonson, B. M. (1985). Sedimentological constraints on the origins of Precambrian iron formations. Geol. Soc. Amer. Bull., v. 96, pp.244-252.